

Method of Estimating the Long-term Rupture Strength of 11Cr-2W-0.4Mo-1Cu-Nb-V Steel

MANABU TAMURA

Long-term rupture data of 11Cr-2W-0.4Mo-1Cu-Nb-V steel were analyzed using an exponential equation for stress regarding time to rupture as a thermal activation process. The fitness was compared with the usually employed method assuming power-law creep. In the exponential method, rupture data are classified into several groups according to the thermal activation process; the activation energy, Q ; the activation volume, V ; then, the Larson–Miller constant, C , values are calculated, and a regression equation is obtained for each data group. The fitness level of the equation was satisfactorily high for each group. The values of Q , V , and C were unusually small for a data group where an unexpected drop in rupture strength was observed. The critical issue is how to comprehend signs of degradation within the short term. We can observe several signs at a creep time of approximately one-tenth of the times of the degradation events. The small values of Q and V indicate that completely softened regions form and creep locally, which is consistent with previous observations. From both metallurgical considerations and the variations of Q and V , it is suggested that the rate of the unexpected drop in strength is mitigated after further long-term creep.

DOI: 10.1007/s11661-015-2784-9

© The Minerals, Metals & Materials Society and ASM International 2015

I. INTRODUCTION

SINCE modified 9Cr-1Mo steel was first industrialized,^[1] many high-Cr heat-resistant steels with high creep strength have been developed.^[2] Some of these steels have been registered by the American Society for Testing & Materials (ASTM) and other authoritative public organizations. These developments have allowed power stations to employ steam conditions higher than 873 K (600 °C) and 30 MPa, thus realizing ultra-super critical power generation and increasing the efficiency of power generation.^[2] With this background, there has been less activity in developing new martensitic steels of high strength, but the long-term rupture testing of high-strength martensitic steels is still necessary. Indeed, it has become more important to estimate the long-term rupture strengths of high-strength martensitic steels because such steels are manufactured day by day, and the allowable tensile stresses of the steels are periodically reviewed.^[3] Many kinds of parameters combining temperature and creep time have been proposed for estimating long-term strength, where fitting curves for estimation were obtained by combining the parameters and stress. Among these parameters, the Larson–Miller parameter (LMP)^[4] has been widely used to estimate long-term rupture strengths of carbon steel and low-alloy steel. Rupture data for periods longer than 100,000 hours have already been published in the data sheet for 0.2 pct carbon steel tubes by the National Institute for Materials Science

(NIMS) (Tsukuba, Japan), and the regression curves obtained using the LMP related to a polynomial of the logarithmic stress fully follow the observed times to rupture.^[5] This successful result is attributed to the fact that the microstructure of carbon steel is stable over a long period.^[6–8] However, some high-Cr martensitic steels with high strength for use in ultra-super critical power stations have been reported to deteriorate unexpectedly in creep testing longer than several tens of thousands of hours.^[9] The deterioration is attributed to localized regions near prior austenitic grain boundaries (PAGB) being preferentially recovered through the formation of Z phase at PAGB accompanying the disappearance of one of the main strengthening factors of the finely dispersed carbonitride (MX, where M denotes metallic elements preferentially forming carbide and/or nitride, and X denotes carbon and/or nitrogen) particles,^[10,11] besides the scavenging effect of solute elements of W and Mo owing to the grain boundary precipitation of Laves phase.^[12,13] It is thus easy to overestimate the long-term strength of these high-strength steels. Kimura *et al.*^[14] proposed for this problem that rupture data below 50 pct of proof stress (0.5PS) at test temperatures are used in the analysis. However, there are still differences between the calculated and observed values, though considerable improvement was confirmed when following their proposal. Therefore, it is concluded that there is still no general method with which to estimate the long-term rupture strength of high-Cr and high-strength heat-resistant steel. The creep data sheet for 11Cr-2W-0.4Mo-1Cu-Nb-V steel was revised in March 2013 by the NIMS.^[15] In the current work, using the data sheet, an estimation method for the long-term rupture strength of high-strength martensitic steel was improved. If the possibility of an unexpected drop in long-term strength

MANABU TAMURA, formerly with the National Defense Academy, Yokosuka, Japan, is now retired. Contact e-mail: mtamura.1943@pep.ne.jp

Manuscript submitted November 2, 2013.

Article published online February 11, 2015

is suspicious in an early stage of creep test, the counter-measures for it can be taken. Therefore, a method for detecting signs of degradation is also discussed using the short-term data.

II. MATERIALS

11Cr-2W-0.4Mo-1Cu-Nb-V steel is equivalent to Gr.122 of the ASTM. The data sheet for this material includes, besides creep data, the manufacturing method, mechanical properties, and microstructures for steel products of pipes [Japanese Industrial Standards (JIS) KA-SUS410 J3 TP], plates, and tubes.^[15] There are no significant differences among the chemical compositions of the three products, excepting that the nitrogen and carbon contents of plates and tubes, respectively, are a little higher than the contents of the other products. The microstructures of the three products are tempered martensite, but pipes contain a very small amount of δ -ferrite. The data sheet includes digital data for not only the time to rupture but also the minimum creep rate (MCR) and times to 0.5, 1, 2, and 5 pct total strains. When data of the time to a specified total strain are used (*e.g.*, the time to 0.5 pct total strain) the word “total” is removed for simplicity.

III. ANALYSIS METHOD

Assuming a thermal-activating process for dislocation glide and subsequent climb to overcome obstacles, the time to rupture is expressed as^[16]

$$t_r = t_{r0} \exp[(Q - \sigma V)/RT], \quad [1]$$

where t_{r0} is a constant, Q is the increase in internal energy owing to creep deformation, σ is the applied stress, V is the activation volume, R is the gas constant, and T is the absolute temperature. The variable t_{r0} correlates with the Larson–Miller constant, C , according to

$$C = \log(1/t_{r0}). \quad [2]$$

The correct meaning of Q is given above, and the meanings of Eqs. [1] and [2] are explained in previous work.^[16] However, Q is usually called simply the activation energy or the activation energy for creep. Here, we call Q the activation energy, for simplicity. Moreover, the applicability of Eq. [1] was confirmed for rupture data of many kinds of heat-resistant steels and alloys.^[17,18] Further, the activation volume is defined as the product of the area swept by dislocations and the length of the Burgers vector when we discuss the microscopic deformation mechanisms by dislocations. However, since it is impossible to measure directly the area swept by dislocations, another interpretation is necessary from a creep-deformation-measuring point of view. From this point of view, Mura and Mori^[19] gave a clear interpretation that σV denotes the value of work done by a specimen toward a loading system, because

the displacement owing to plastic deformation is determined by the total amount of moving dislocations swept out of a specimen in an activation process. The work done by the specimen is

$$\sigma V \equiv W\Delta L = \sigma S\Delta L \quad \text{or} \quad S\Delta L = V, \quad [3]$$

where W , ΔL , and S are the applied load, displacement, and cross section of a specimen, respectively. Therefore, the activation volume is a measure of creep deformation during an activation process.

Apart from Eq. [1], analysis based on Norton's law,^[20] which gives the relation of $\log t_r \propto \log \sigma$, is widely accepted. In the analysis, a temperature-compensated time such as the LMP, $P = T(\log t_r + C)$, is used instead of $\log t_r$. Even if the temperature-compensated time is used, a linear relationship between $\log \sigma$ and the temperature-compensated time hardly holds. Therefore, this study employs the cubic equation:^[16]

$$P = T(\log t_r + C) = a_0 + a_1 \log \sigma + a_2 \log^2 \sigma + a_3 \log^3 \sigma, \quad [4]$$

where a_i are constants.

Applying Eq. [1] or [4] to the observed times to rupture, material constants for each equation were obtained by multiple regression analysis. Three constants, Q , V , and C , are obtained for Eq. [1] (hereinafter, we call this calculation method the exponential-law method) and five constants, a_i and C , are obtained for Eq. [4] (hereinafter, we call this method the power-law method).

Using the obtained constant, C , the LMP for individual time to rupture, P_i , can be calculated. Now, we define a new variable, Q' , as

$$Q' = 2.3R(P_i)_{\text{avg}}, \quad [5]$$

where the subscript “avg” denotes average.

Incidentally, combining Eqs. [1] and [2], we obtain the LMP

$$P = T(\log t_r + C) = (Q - \sigma V)/2.3R. \quad [6]$$

Comparing Eqs. [5] and [6], Eq. [5] can be developed as

$$Q' = 2.3R(P_i)_{\text{avg}} = (Q - \sigma V)_{\text{avg}}. \quad [7]$$

The correct meaning of $(Q - \sigma V)$ in Eq. [1] is the enthalpy change for an activation process. However, $(Q - \sigma V)$ is usually treated as the activation energy, because this term is calculated similar to the activation energy of an Arrhenius plot. Therefore, we call $(Q - \sigma V)$ in Eq. [1] the apparent activation energy distinguishing from Q in this study. In any event, both $(Q - \sigma V)_{\text{avg}}$ and $(Q - \sigma V)$ formally hold the same meaning. Therefore, we can refer to Q' as the apparent activation energy. In other words, we can say that the value corresponding to the apparent activation energy can be calculated even for the power-law method.

It should be evaluated which model equation, Eq. [1] or [4], is adequate for fitting actual data. In multiple regression analysis, one of the indicators of fitness for a given set of data is a coefficient of determination, r^2 , but we use r , a correlation coefficient, for simplicity. In multiple regression analysis, it is assumed that data of a population are mutually independent and are distributed normally around the mean value. Therefore, in the case of the power-law method, multiple regression analysis is significant if a population of the LMPs for individual data, P_i s, sufficiently covers the LMP for a target of the developed material. In many cases, this criterion is satisfied. However, in the case of estimating the strength after 100,000 hours, reducing the difference between the calculated value and an actual data point near 100,000 hours is a critical issue. In this sense, the estimated maximum time-to-rupture ratio, R_{mtr} , is newly defined as

$$R_{mtr} = (t_{rcal}/t_{robs})_{mtr}, \quad [8]$$

where t_{robs} and t_{rcal} are the observed maximum time to rupture and the calculated time to rupture under a condition of the observed data, respectively. The value of R_{mtr} is also taken into account as an indicator of the fitness.

IV. RESULTS OF ANALYSIS OF TIME TO RUPTURE

A. Evaluation of Regression Equations

1. Analysis employing the power-law method

Figure 1 is a conventional plot of stress vs time to rupture for pipes of 11Cr-2W-0.4Mo-1Cu-Nb-V steel. Broken lines in Figure 1 show regression lines obtained using the power-law method for all data. The optimized value of C is shown in the figure. The fitness of the equation appears reasonable ($r = 0.977$), but maximum times to rupture at a temperature range of 873 K to 923 K (600 °C to 650 °C) shown by diamond marks are far short of the regression lines. On the other hand, solid regression lines are given for the data below 0.5PS

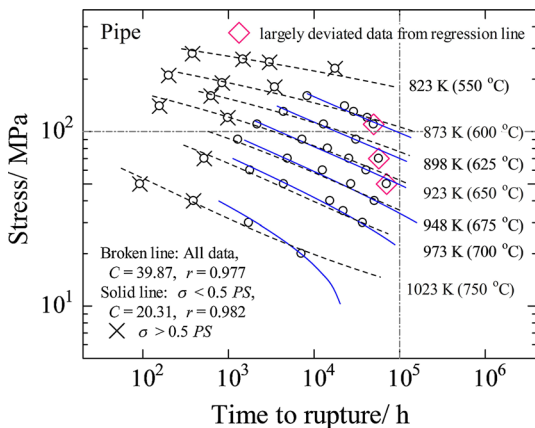


Fig. 1—Stress vs time to rupture for the steel pipes and regression lines obtained employing the power-law method.

according to Kimura's proposal.^[14] The correlation coefficient improves from 0.977 to 0.982 and the estimated maximum time-to-rupture ratio, R_{mtr} , at 873 K, 898 K, and 923 K (600 °C, 625 °C, and 650 °C) certainly improve from 1.60, 2.83, and 1.80 to 1.16, 1.77, and 1.38, respectively, when using a 0.5PS criterion. However, data points shown by diamonds are still considerably short of the solid lines, or the strength is overestimated. The time to rupture of 0.2 pct carbon steel (JIS STB 410) already exceeds 100,000, and the 100,000-hours rupture strength is listed using the LMP and a quartic equation of the logarithm of stress.^[5] Using these values, the values of R_{mtr} at 673 K and 723 K (450 °C and 400 °C) after 100,000 hours are calculated as approximately 1.36 and 1.0, respectively. The values of R_{mtr} of the carbon steel are close to unity because the microstructure of carbon steel generally changes slowly,^[6-8] not because a higher-degree regression equation is used instead of Eq. [4]. Therefore, the higher values of R_{mtr} for 11Cr-2W-0.4Mo-1Cu-Nb-V steel suggest that there may be drastic changes in microstructure around 873 K (600 °C) after several tens of thousands of hours, which causes the unexpected drops in creep strength. When we evaluate the long-term rupture strength after 100,000 hours, the longest data points shown as diamond marks in Figure 1 should be more heavily weighed. Therefore, it is natural that the fitness of the regression equation is improved when short-term data are excluded according to the criterion of $\sigma < 0.5PS$ as shown in Figure 1. However, backgrounds for imposing a specified restriction on a population of creep data to improve the fitness of long-term creep data are not clear, and an approach like this is considered to be based on a limited argument.

2. Analysis employing the exponential-law method

According to the thermally activated process expressed by Eqs. [1] and [2], a similar event to the time to rupture, observed at 898 K (625 °C) and 70 MPa after 57,095 hours, for example, should take place at a higher temperature and/or within a shorter time. In the exponential-law method, a relation between the stress and time to rupture is presented on a semi-logarithmic plot as shown by Eq. [6]. Figure 2 shows a semi-logarithmic plot for the same data as in Figure 1. In the exponential-law method, data are first classified into several groups where the same material constants, Q , V , and C , are shared in each group. From Eq. [1], we obtain

$$\log t_r + C = (Q - \sigma V)/2.3RT. \quad [9]$$

Partially differentiating Eq. [9] at a constant temperature, we obtain

$$-\partial\sigma/\partial\log t_r|_T = 2.3RT/V, \quad [10]$$

which indicates that data for the same temperature in a specified group are presented linearly with a slope of $2.3RT/V$ as shown in Figure 2. In this paper, the "slope" of a stress vs log time relation has a positive value. Since the slope of $2.3RT/V$ varies little with

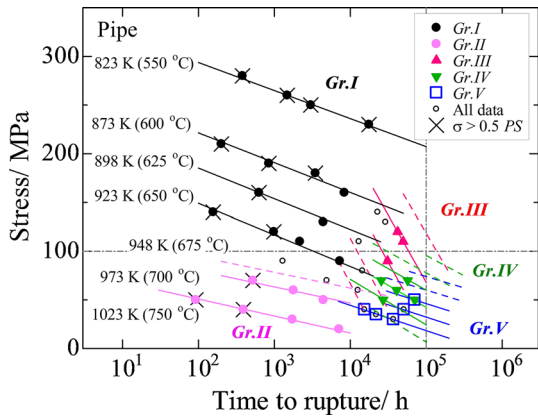


Fig. 2—Stress vs time to rupture for the steel pipes analyzed employing the exponential-law method and regression lines for each data group. Broken lines are extrapolated for temperatures where data are lacking.

temperature, a nearly parallel relationship is found within the same group. This relation can be easily found using a single transparent ruler. In this way, we can define data groups *Gr. I* and *Gr. II*, temporarily. Applying Eq. [1] or [9] to *Gr. I* and *Gr. II*, Q , V , and C are obtained by regression analyses. Using these material constants, linear regression lines are drawn in Figure 2. Among the data shown by open circles, which were originally not judged to belong to *Gr. I* or *Gr. II*, rupture data for 923 K (650 °C) and 80 MPa and for 948 K (675 °C) and 70 and 60 MPa seem to belong to *Gr. I* and *Gr. II*, respectively. A broken line parallel to the 973-K (700 °C) line is an extrapolated line for 948 K (675 °C).

In terms of long-term data, Figure 2 shows that rupture strength at 873 K (600 °C) begins to decrease rapidly, or the slope, $-\partial\sigma/\partial\log t_r$, increases suddenly after about 20,000 hours. A rapid decrease in strength like this is easily found from a semi-logarithmic plot like the one shown in Figure 2 rather than by a log-log plot like the one shown in Figure 1. Two long-term rupture data at 873 K (600 °C) shown by solid triangles are defined as *Gr. III*. Candidate data at 898 K (625 °C) for *Gr. III* are the longest and the second-longest data points. Three long-time rupture data at 973 K (700 °C) are defined as a data group, *Gr. V*, indicated by square marks in Figure 2. Moreover, the longest data points at 973 K, 948 K and 923 K (700 °C, 675 °C, and 650 °C) seem to be evenly spaced, and they therefore belong to *Gr. V*. Long-term rupture data which belong to between *Gr. III* or *V* are temporarily defined as *Gr. IV*. Turning to *Gr. III*, the slopes of data at 873 K and 898 K (600 °C and 625 °C) are different, and, so, either the data point corresponding to 90 MPa or that corresponding to 70 MPa at 898 K (625 °C) belongs to *Gr. III*. Therefore, we can classify long-term rupture data into several cases as populations for *Gr. III* and *IV*. To examine the temporarily defined *Gr. III* and *IV* using a ruler, the activation energy for each case was calculated according to Eq. [9]. The activation energies in any case for *Gr. III* and *IV* are considerably lower than those for *Gr. I*, *II*, and *V*, and moreover, some are even lower than the

activation energy of the self-diffusion of α -Fe (256 kJ/mol).^[21] There is no absolute evaluation criterion with which to select the best case. However, among the cases examined, the results shown in Figure 2 are judged to be most reasonable for the following reasons. Primarily, the degree of degradation (*i.e.*, the slope) in Figure 2 tends to moderate from *Gr. III* to *Gr. V*, and therefore, the activation energy should vary inversely. Second, the value of Q for creep should be close to the activation energy of the self-diffusion of α -Fe. Even in this case, the activation energies for *Gr. III* and *IV* are similar to or smaller than that for the self-diffusion of α -Fe. Under these test conditions, there was an unexpected drop in rupture strength, and this should be because of the drastic changes in microstructure. Therefore, we refer to rupture data in *Gr. III* and *IV* as “material degradation data”.

Broken lines near 100,000 hours and 100 MPa are drawn for *Gr. III* and *IV* at a temperature of 848 K (575 °C). Figure 2 shows that the deformation mechanism varies with time. For example, at 898 K (625 °C) after *Gr. I* corresponding to the early stage, there is rapid degradation from about 20,000 hours through 40,000 hours (*Gr. III*), after which there is slower degradation (*Gr. IV*). At 923 K (650 °C), *Gr. IV* follows *Gr. I*, while *Gr. III* is absent, and after about 70,000 hours, the degradation rate seems to decrease further (*Gr. V*). However, at 873 K (600 °C), following *Gr. I*, there is an unexpected and drastic decrease in the rupture strength under the conditions of decrease from 140 to 110 MPa (about 20,000 hours, *Gr. III*). Further rupture data have not yet been obtained; however, the assumption of a thermally activated process implies that a rupture phenomenon of *Gr. IV* observed at 898 K (625 °C) should be reproduced after a longer time at 873 K (600 °C). Therefore, there should be deformation mechanisms of *Gr. IV* or *V* even at a temperature of 873 K (600 °C) along the broken lines drawn near 100,000 hours and beyond, and it is thus evaluated that the drastic decrease in rupture strength observed at 873 K (600 °C) around 20,000 to 40,000 hours will be mitigated rapidly after about 80,000 hours.

Figure 2 shows that the three maximum times to rupture data indicated by diamonds in Figure 1, which are far below the regression lines, do not belong to the same data group, but belong to *Gr. III*, *IV*, and *V*, respectively. Further, Figure 2 indicates that data at 898 K (625 °C) paired with the data of *Gr. III* at 873 K (600 °C), which show a drastic decrease in rupture strength, are not the longest data points but the second-longest data points at 898 K (625 °C) and 90 MPa. In Figure 1, regression analysis using the power-law method was also carried out for the limited data of $\sigma < 0.5PS$ to improve fitness. In addition, in Figure 2, \times -marks denote the data of $\sigma > 0.5PS$, and it is found that the region for the data of *Gr. III* and *IV* and/or *Gr. V* is further restricted by the limitation of $\sigma < 0.5PS$.

3. Evaluation of fitness of regression equations

In evaluating the fitness of a power-law equation, Eq. [4], or an exponential equation, Eq. [1] or [9], it is a problem how the estimated value is close to the observed

values near 100,000 h, which is the basis of calculating allowable stresses. The rupture data point at 898 K (625 °C), 70 MPa, and 57,095 hours, which was farthest from the regression line in Figure 1, was selected as a target for evaluation. Analyses were carried out for the cases shown in Figure 2 using the exponential-law method, and the correlation coefficient, r ; the estimated maximum time-to-rupture ratio, R_{mtr} ; the activation energy, Q ; the activation volume, V ; the Larson–Miller constant, C ; the apparent activation energy, Q' ; and the number of data are listed in Table I. All analyses were carried out for *Gr. IV*, because the target rupture data belonged to *Gr. IV*. In the calculation using the power-law method, all data and the selected data of $\sigma < 0.5PS$ were analyzed, and the results are given in Table I. For the exponential-law method, the correlation coefficient and the estimated maximum time-to-rupture ratio are $r = 0.995$ and $R_{mtr} = 1.04$, respectively. The fitness of the power-law method was improved by selecting rupture data of $\sigma < 0.5PS$ as $r = 0.982$ and $R_{mtr} = 1.77$, but these values are far inferior to those of the exponential-law method. In the calculation using the exponential-law method, only rupture data of *Gr. IV* (i.e., the material degradation data explained above) are used. Conversely, in the calculation using the power-law method, as shown in Figure 1, not only the material degradation data but many other rupture data were analyzed in the case of $\sigma < 0.5PS$, and so, the indicators listed in Table I were difficult to improve remarkably. Therefore, the fitness of the exponential-law method is superior to that of the power-law method.

4. Analysis results for plates and tubes

It was suggested in Section IV–A–2 that a trend of a drastic decrease in rupture strength observed near 40,000 hours in the *Gr. III* region of the steel pipes shown in Figure 2 would weaken at longer times owing to changes in the deformation mechanism from *Gr. III* to *Gr. IV*. However, the number of data points at 873 K (600 °C) is limited to only two, and therefore, the question that the change is because of the scattering of

observed values during testing cannot be denied. Analyses of steel plates and tubes with manufacturing processes different from those of the steel pipes were thus performed.

Classification of rupture data and the subsequent analysis of steel plates and tubes made of 11Cr-2W-0.4Mo-1Cu-Nb-V steel were performed similar to the classification and analysis shown in Figure 2 using the exponential-law method. Though the definition of a population of each data group is not the same among pipes, plate, and tubes, all rupture data for each product can be classified into *Gr. I to V*. A steep slope in a plot of stress vs log time to rupture was again observed for plates and tubes in *Gr. III* at 873 K (600 °C), although the number of data is again limited to only two or three.

Table II shows the activation energy for each group of three kinds of steel products, which summarizes the characteristics of each data group. Although, in a strict sense, comparing the values of Q among three products is not meaningful, it is confirmed from Table II that the values of Q for *Gr. I, II, and V* are rather large, and the values of Q for *Gr. III and IV* corresponding to the material degradation data are rather low and that the activation energy of steel tubes is larger than that of the self-diffusion of α -Fe, but is still much lower than the activation energies of *Gr. I and II*.

It was confirmed that, through the analyses similar to those in Figure 2, although the corresponding figures are omitted, at 898 K (625 °C), the deformation mechanism changes from the one for *Gr. I* on the high-stress side, through the one for *Gr. III*, to the one for *Gr. IV* in any case of pipe, plate, or tube. Although rupture data below 100 MPa have not yet been obtained at 873 K (600 °C), a deformation mechanism at this temperature after approximately 100,000 hours or longer should vary as the deformation mechanism of *Gr. IV* or *V* according to the assumption of the thermally activated process, and thus, the time to rupture at 873 K (600 °C) will follow the broken lines shown in Figure 2. Therefore, it is reasonable to conclude that a drastic decrease in the rupture strength of *Gr. III* finishes within a limited range and the rupture strength will subsequently vary in a gentle manner.

B. Estimation of Rupture Strength Using Short-Term Data

As shown in Figure 2, rupture data of the steel pipes within 10,000 hours can be classified into two groups: *Gr. I and II*, and linear relationships are confirmed in a semi-log plot. However, beyond 10,000 hours, obvious

Table I. Comparison of Fitness Between the Exponential-Law Method and the Power-Law Method (For All Data and Data $\sigma < 0.5PS$) for the Data Points of 57,095 h at 898 K (625 °C) and 70 MPa of the Steel Pipes and Variations of Q , V , C , Q' , and n for Each Dataset

	Exponential Law	Power Law	
		All Data	<0.5PS
Q (kJ/mol)	271.6		
V (cm ³ /mol)	387.9		
C	9.46	25.20	20.31
Q' (kJ/mol)	244.2	509.0	435.0
n number of data	5	40	27
R_{mtr} at 898 K (625 °C), 70 MPa	1.04	2.83	1.77
r	0.995	0.977	0.982

The exponential-law analyses were made on a *Gr. IV* dataset, which included rupture data at 898 K (625 °C) and 70 MPa.

Table II. Variation in the Activation Energy for Each Data Group of the Steel Pipes, Plates, and Tubes

kJ/mol	Pipe	Plate	Tube
<i>Gr. I</i>	809.9	799.4	825.6
<i>Gr. II</i>	723.7	685.8	842.0
<i>Gr. III</i>	221.1	241.4	382.7
<i>Gr. IV</i>	272.6	324.0	339.6
<i>Gr. V</i>	399.8	437.9	436.3

gaps between the observed values and the regression lines for *Gr. I* appear, and at about 23,000 hours, a gap is clearly identified even at 873 K (600 °C), a temperature at which there is a dramatic decrease in rupture strength. No later than about 30,000 hours, an obvious decrease in rupture strength was confirmed over a wide temperature range of 873 K to 923 K (600 °C to 650 °C). Therefore, the difference between the existing rupture data at 898 K (625 °C) and 70 MPa after 57,095 hours and the rupture strength estimated using short-term data, within 10,000, 23,000, and 30,000 hours, should be confirmed. This data point is the longest among the material degradation data. Rupture strength was also estimated employing the power-law method and $\sigma < 0.5PS$ data.

Figure 3 shows an example of analysis employing the exponential-law method and rupture data points shorter than 30,000 hours. Although rupture data of *Gr.s. I* and *II* in Figure 3 are the same as those in Figure 2, the structure of data of *Gr.s. III* and *IV* in Figure 3 differs from that of *Gr.s. III* and *IV* in Figure 2. *Gr. III* in Figure 3 was constructed from data at 873 K, 898 K, and 923 K (600 °C, 625 °C, and 650 °C), and *Gr. IV* was constructed from long-term data other than *Gr.s. I, II, and III*. Data points longer than 30,000 hours and a target data point for estimation are indicated by plus marks and a star mark, respectively. Near the target test condition, a deformation mechanism of *Gr. IV* is judged to dominate; the rupture strength was estimated using *Gr. IV* data and the estimated maximum time-to-rupture ratio, R_{mtr} , defined by Eq. [8] for *Gr. IV* is $R_{mtr} = 1.51$, and this value is far inferior to $R_{mtr} = 1.04$ obtained using the degradation data presented in Table I.

Similar analyses to the results presented in Figure 3 were made for data within 10,000 and 23,000 hours, and the results are summarized in Figure 4. The vertical axis of Figure 4 shows the estimated rupture strength at 898 K (625 °C) for 57,095 hours, where the actual creep stress was 70 MPa. The horizontal axis shows the maximum time to rupture, and the results obtained using all data are plotted at 70,519 hours, which is the maximum time to rupture at 923 K (650 °C). Figure 4 shows that although an extremely high rupture strength

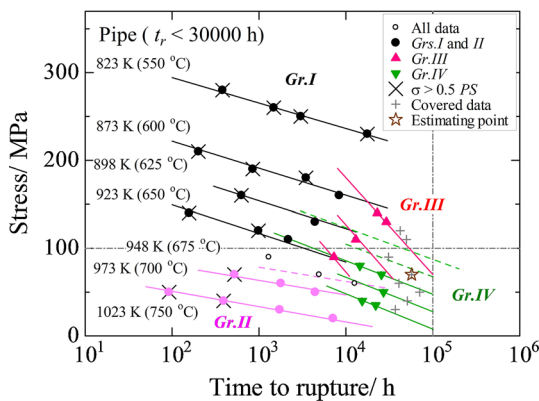


Fig. 3—Stress vs time to rupture for the same steel pipes as in Fig. 2, but rupture data for analysis are limited to data points shorter than 30,000 h.

at 898 K (625 °C) and for 57,095 hours (*i.e.*, about 30 pct higher than the actual stress of 70 MPa) is estimated employing the exponential-law method for $t_r < 10,000$ hours, the estimation accuracy improves by +13 pct when we have the data for $t_r < 23,000$ hours and by a further +9 pct when we have the data for $t_r < 30,000$ hours, where there is obvious degradation. However, the power-law method gives strength that is about 20 pct higher even for $t_r < 30,000$ hours. The estimation results shown in Figure 4 imply that the exponential-law method is superior to the power-law method for extrapolation when a sign of degradation is clearly recognized; however, obtaining longer times to rupture data over the completion of a drastic decrease in rupture strength, data for 100,000 hours for example, is a requirement for further precise estimation of the long-term rupture strength of material that experiences unexpected degradation in a long-term test as shown in Figure 2.

Most of the material degradation data, *Gr.s. III* and *IV* shown in Figure 2, were recorded for times exceeding 30,000 hours. The rupture strength estimated at 898 K (625 °C) and for 57,095 hours employing the power-law method and rupture data points longer than 30,000 hours and $\sigma < 0.5PS$ are shown as a square mark in Figure 4. This value is strangely similar to the value estimated by the exponential-law method. This similarity could be interpreted as the estimation strength not depending on the calculation method (*i.e.*, the exponential-law method or the power-law method) if the analysis data mainly comprise material degradation data. However, these results shown in Figure 4 should be a casual coincidence, because there is no rational reason to restrict analysis data to $t_r > 30,000$ hours and $\sigma < 0.5PS$. Furthermore, the exponential-law method can take metallurgical considerations into account, and therefore, the exponential-law method is considered to be better than the power-law method in increasing the fitness of the rupture data or estimating long-term rupture strength.

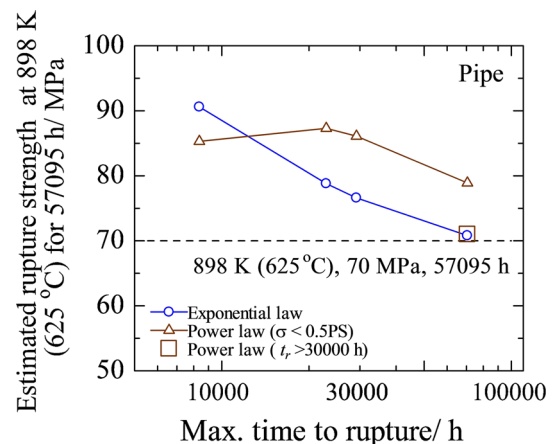


Fig. 4—Rupture strength at 898 K (625 °C) after 57,095 h estimated, employing the exponential- or power-law method and limited data as a function of maximum time to rupture for the steel pipes. Strength estimated using the power-law method for $t_r > 30,000$ h is also plotted.

C. Extrapolation to 100,000 hours

The above sections discussed the type of model equation suitable for existing long-term rupture data and the exactness of the estimate of existing long-term rupture data using short-term data. However, it is an interesting problem to determine for how much longer time strength can be estimated. The exponential-law method has an advantage that, in addition to the calculation being based on a thermally activated process, the results can be evaluated by metallurgical considerations. It was estimated from Figure 2 that the deformation mechanism varies from *Gr. III* to *Gr. IV* or *V* in a long-term region at 873 K to 923 K (600 °C to 650 °C). Figure 5 is an enlarged view of the long-term region presented in Figure 2. In Figure 5, the regression curves for 873 K to 923 K (600 °C to 650 °C) obtained using the power-law method and long-term data of $t_r > 30,000$ hours are also drawn. These regression lines or curves reveal that the 100,000-hours rupture strengths at 873 K, 898 K, and 923 K (600 °C, 625 °C, and 650 °C) are estimated approximately as a little under 80 MPa, about 60 MPa, and a little over 40 MPa, respectively, and the estimated values do not heavily depend on the analysis model (*i.e.*, the exponential- or power-law method).

The values of MCR at low stresses are also given in the data sheet of 11Cr-2W-0.4Mo-1Cu-Nb-V steel,^[15] but the corresponding rupture data at low stresses are not yet listed. Time-to-rupture data corresponding to these MCR values can be estimated using the Monkman-Grant relation.^[22] The obtained time-to-rupture data are plotted by diamond marks in Figure 5. Two rupture data estimated from the MCR at 873 K (600 °C) support the validity of estimating the 100,000-hours rupture strength from the regression line of *Gr. IV* (inverse triangles) or *Gr. V* (squares) and not a regression line of *Gr. III*. However, Figure 5 shows that according to the abovementioned consideration at 923 K (650 °C), the time to rupture may be overesti-

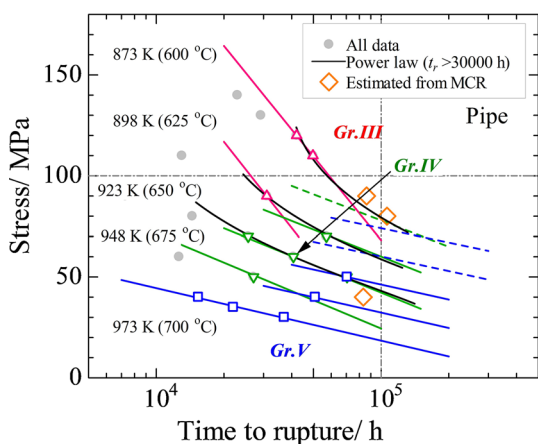


Fig. 5—A long-term portion of stress vs time to rupture for the steel pipes and regression lines for *Gr. III*, *IV*, and *V* analyzed employing the exponential-law method and regression curves obtained employing the power-law method. Broken lines are extrapolated for temperatures where data are lacking. Diamonds indicate estimates made using the minimum creep rate.

mated from the MCR. Long-term rupture data points longer than 100,000 hours have not yet been obtained. Therefore, to eliminate this uncertainty, it is necessary to continue long-term creep rupture tests.

Figure 5 shows that the 100,000-hours rupture strengths estimated employing the power-law method and the rupture data of $t_r > 30,000$ hours eventually and approximately coincide with those estimated using the exponential-law method. However, it is noteworthy that the extrapolated rupture strength largely varies depending on the construction of data in the case of the power-law method. Figure 6 shows regression curves obtained using the power-law method and data of $\sigma < 0.5PS$, $t_r > 30,000$ hours, and $t_r > 42,000$ hours. The figure reveals that the values extrapolated to 100,000 hours vary with the population of data and the 100,000-hours rupture strength decreases in the order of $\sigma < 0.5PS$, $t_r > 42,000$ hours, and $t_r > 30,000$ hours. The regression lines for $t_r > 30,000$ hours in Figures 5 and 6 appear different, owing to the difference in the y-axis; *i.e.*, a linear vs logarithm axis. The apparent activation energy shown in the figure varies with the 100,000-hours rupture strength in the same order as shown in the figure. In the figure, a boundary between *Gr. I, II*, and *V* and *Gr. III* and *IV* (see Figure 2) is drawn. The rough coincidence in the estimated strength shown in Figure 5 may be because of overlapping of the data regions of *Gr. III* and *IV* and $t_r > 30,000$ hours. It is reasonable in a sense that the apparent activation energies for $\sigma < 0.5PS$ and $t_r > 30,000$ hours shown in Figure 6 are between those of *Gr. I to V* and *Gr. III* and *IV*, referring to Tables I and II. However, it is strange that the apparent activation energy for $t_r > 42,000$ hours is higher than the activation energy of *Gr. III* or *IV*. This strangeness may come from the uncertainty of the meaning of Eq. [4]. It can be said that, although the power-law method is reasonable in improving curve fitting for the existing data of material, it is not an

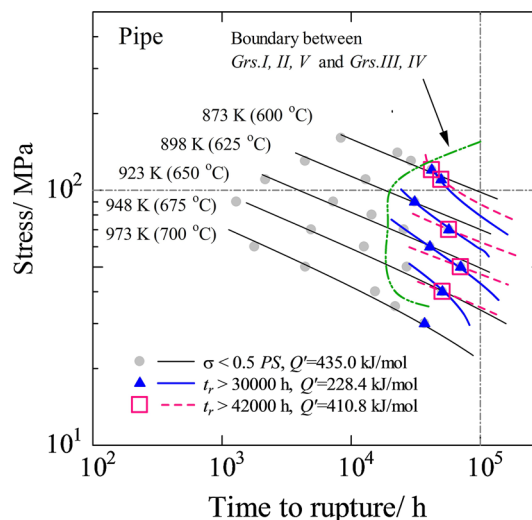


Fig. 6—Variations in regression lines obtained employing the power-law method because of the different databases of the steel pipes. The boundary between *Gr. I, II*, and *V* and *Gr. III* and *IV* in the exponential-law method (see Fig. 2) is also indicated.

adequate procedure with which to extrapolate the long-term strength of material that undergoes a drastic change in microstructure and subsequently a degradation in strength.

V. DETECTION OF SIGNS OF CREEP DEGRADATION

A. Variations in Q and V During Creep Deformation

The rupture strengths of several high-strength martensitic steels decrease unexpectedly at approximately 873 K (600 °C) after several tens of thousands of hours. It has been explained that the exponential-law method outperforms the power-law method in evaluating the 100,000-hours rupture strength of 11Cr-2W-0.4Mo-1Cu-Nb-V steel. However, rupture data points longer than 30,000 hours are needed, and moreover, the inclusion of the degradation data in a population is an absolute requirement for predicting the 100,000-hours rupture strength with high accuracy even when using the exponential-law method. Conversely, obtaining rupture data over 30,000 hours requires a very long time following the preliminary completion of alloy development. Fortunately, the data sheet^[15] provides detailed information on creep curves such as the time to 0.5 pct strain. Therefore, these data were used to investigate further how the rupture behavior after a long time can be estimated within a short time and to what extent we can get a sign of creep degradation.

Figure 7 shows the analysis results for time to 0.5 pct strain of 11Cr-2W-0.4Mo-1Cu-Nb-V steel pipes obtained employing the exponential-law method. In this analysis, data for the same test conditions as those employed for the rupture data groups shown in Figure 2 were classified into the same group names. However, the following cases were found occasionally. Rupture data at 923 K (650 °C) and 120 to 90 MPa were classified into *Gr. I* as shown Figure 2, but gaps were found in Figure 7. Therefore, re-classification was conducted in a

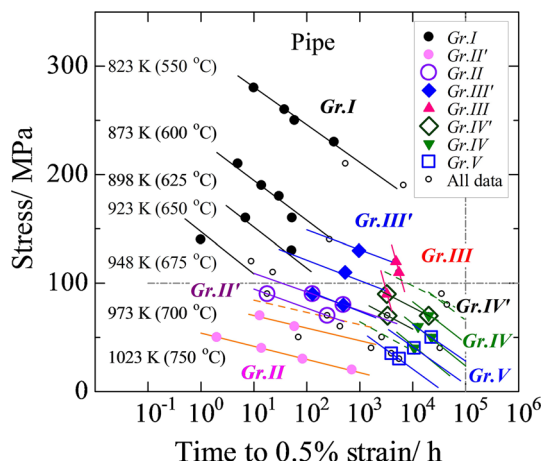


Fig. 7—Stress vs time to 0.5 pct strain for the steel pipes analyzed employing the exponential-law method and regression lines for each data group. Broken lines are extrapolated for temperatures where data are lacking.

manner such that each group has exactly the same test conditions for times to 0.5, 1, 2, 5 pct strain, and rupture. In the new classification, data were fundamentally separated into five groups similar to *Gr. I–V* as shown in Figure 2. However, the new classification included *Gr. II'* for intermediate temperatures of *Gr. I* and *II*, *Gr. III'* for a connecting region between *Gr. I* and *III*, and *Gr. IV'* for a connecting region between *Gr. IV* and *V*. This work considered that (1) as many data as possible are classified into data groups (*i.e.*, there are as few unclassified data as possible); (2) there are at least four data in each group to mitigate scattering error; and (3) the correlation coefficient for each group is higher than 0.99. In Figure 7, data plotted as small open circles could not be classified into any group, because rupture data corresponding to 823 K (550 °C) and 210 and 190 MPa shown in Figure 7 have not yet been obtained. Concerning *Gr. III* and *IV*, a common combination of more than three data could not be found, and so, the number of data per group is limited to three.

Comparing Figure 2 with Figure 7, it is found that the stress dependence of time to rupture and that of time to 0.5 pct strain for each of *Gr. I*, *II*, *III*, *IV*, and *V* are similar and that there is a phenomenon for time to 0.5 pct strain in Figure 7 that is similar to the drastic strength drop for time to rupture in Figure 2. Therefore, if these strength drop phenomena have the same cause, a sign for the unexpected decrease in rupture strength after about 40,000 hours can be detected within a very short time of approximately one-tenth of the time of the event. Analyzing times to specified strain such as those in Figure 7, the variations in Q , V , and C for each data group can be understood as functions of strain and/or time. Figure 8 shows the relation between Q and creep time, where creep time is defined as the geometric mean of creep times within each data group. Figure 8 shows that the activation energies for *Gr. III* to *V* are relatively low (200 to 500 kJ/mol; Q for *Gr. III* is especially low from the beginning of creep) compared with *Gr. I* to *III'*. The small value of Q for *Gr. III* shown in Figure 8 can be recognized within 10,000 hours like the variation in time to 0.5 pct strain shown in Figure 7, and therefore, variation in the activation energy can be used as a sign for the long-term drop in strength. The Larson–Miller constant, C , is strongly correlated with Q ^[16], and the description concerning C is thus omitted. Figure 9 shows the correlation between the activation volume and creep time. The activation volume of *Gr. III*, which is correlated with a drastic decrease in rupture strength, is extremely low, below 200 cm³/mol, during the whole period of creep, and this sign can be detected in a very early time of creep. Since creep time is plotted in a semi-logarithmic style when employing the exponential-law method as shown in Figures 2 and 7, the activation volume is strictly and inversely proportional to the slope, $-\partial\sigma/\partial\log t$, according to Eq. [10], and therefore, the activation volume can be calculated from a set of creep tests at a constant temperature. That is, if a small value of the activation volume is detected within a short time by analyzing creep curves that are observed at a target temperature and under near-target stresses, it will be the most convenient indicator with which to

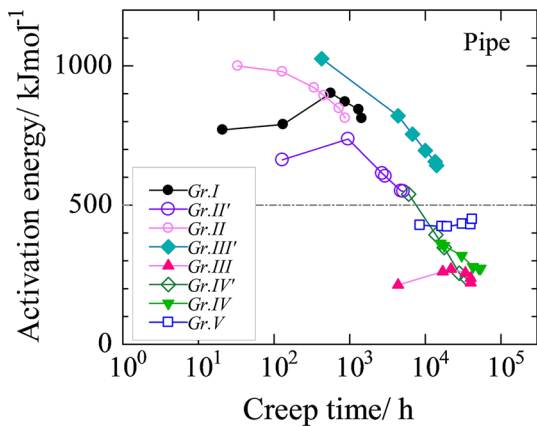


Fig. 8—Variation in the activation energy for each data group of the steel pipes analyzed employing the exponential-law method as a function of creep time.

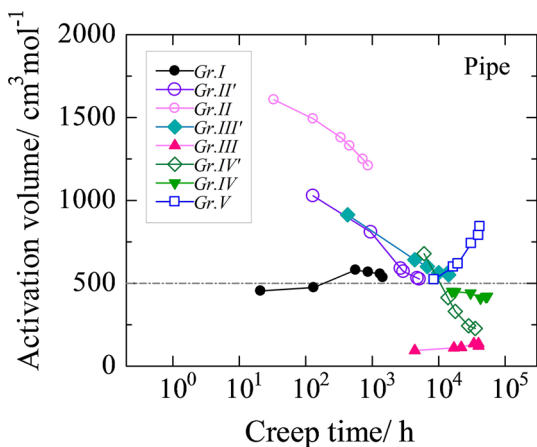


Fig. 9—Variation in activation volume for each data group of the steel pipes analyzed employing the exponential-law method as a function of creep time.

detect a drastic decrease in rupture strength that will occur after several tens of thousands of hours.

B. Time to Small Strain and Time to Rupture vs Stress Diagrams

In the previous section, it was shown that nearly 10,000 hours of creep time is necessary to detect a sign of an unexpected drop in rupture strength, if we assume the strength drop will happen when Q or V in an early stage of creep is less than 500 kJ/mol or 500 cm³/mol, respectively. However, can we further shorten the time required to detect a sign shorter than 10,000 hours?

Figure 10 shows the relationship between the time to rupture and time to 0.5 pct strain. The slope of *Gr. II* in a high-temperature region is less than that of *Gr. I* in a low-temperature region. In general, at the beginning of transient creep, the total creep strain is low at high temperatures and low stresses,^[23] and therefore, time to 0.5 pct strain of *Gr. II* is longer than that of *Gr. I* for the same time to rupture. That the regression line for *Gr. II*

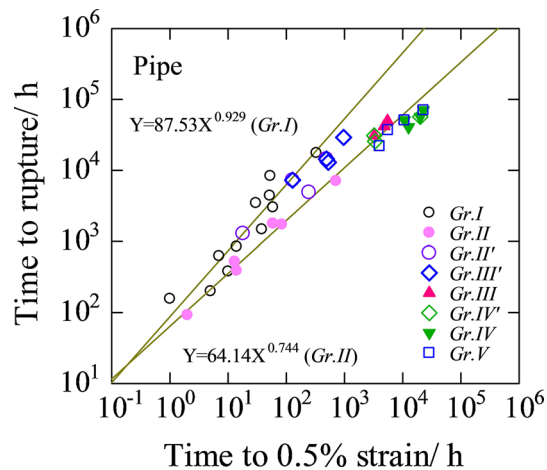


Fig. 10—Correlation between time to 0.5 pct strain and rupture for the steel pipes. Classification of data and the naming of each group are given in Fig. 7.

fits the data points of *Gr. III* can be interpreted as the recovery progressing rapidly in a *Gr. III* region and creep behavior being similar to that above 973 K (700 °C), even though *Gr. III* has a lower temperature of 873 K (600 °C). Data of *Gr. III'* begin to deviate from the regression line for *Gr. I*. Therefore, detailed analyses conducted to explain why *Gr. III'* deviates from *Gr. I* should provide a sign of an unexpected strength drop. However, since this figure can only be valid after all rupture data are prepared, this discussion is meaningless.

To search for a sign from another point of view, Figure 11 shows the relation among time to rupture and times to 0.5 and 1 pct strain at 873 K (600 °C) for the steel pipes. In the figure, regression lines of *Gr. I*, *III'*, *III*, and *IV'* shown in Figures 2 and 7 are drawn. Regression lines for 1 pct strain are easily obtained in a similar manner shown in Figure 7 and are drawn in the figure. As mentioned above, an unexpected drop in strength was already observed at 0.5 pct strain between 120 and 110 MPa for the steel pipes. However, the slope, $-\partial\sigma/\partial\log t$, for time to 0.5 pct strain of *Gr. III'* observed between 140 and 120 MPa is less than that of not only *Gr. III* but also *Gr. I*. This means that there should be some kind of hardening for *Gr. III'*, compared with *Gr. I*. Therefore, the creep behavior at 873 K (600 °C) of time to 0.5 pct strain of the steel pipes can be understood chronologically such that there is first hardening between 140 and 120 MPa for *Gr. III'* and then rapid softening between 120 and 110 MPa for *Gr. III*, and further, the trend of rapid softening is mitigated for *Gr. IV'*. A similar phenomenon is recognized for time to 1 pct strain. Conversely, concerning time to rupture, a hardening period seems to be buried beneath *Gr. I* and *III* and rapid softening of *Gr. III* seems to appear suddenly after *Gr. I*. The activation volume for time to rupture of *Gr. I* as shown in Figure 9 (the right end) is larger than that for time to 0.5 pct strain (the left end), which corresponds to an inverse slope for time to rupture of *Gr. I* that is slightly less than that for time to 0.5 pct strain. In other words, hardening or subsequent

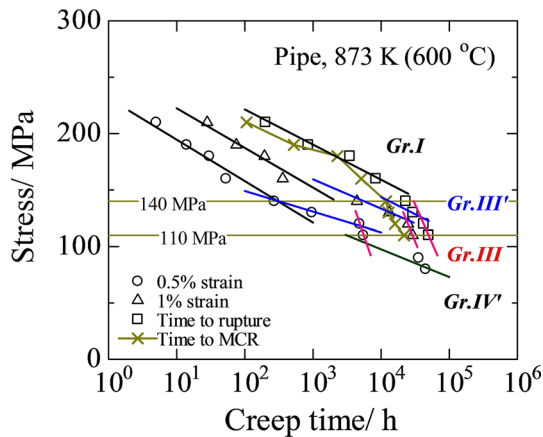


Fig. 11—Times to rupture, 0.5 pct strain, 1 pct strain, and MCR vs stress relation at 873 K (600 °C) for the steel pipes.

softening occurs for the *Gr. I* data themselves. This is supported by Figure 8 of the activation energy of *Gr. I*. Figures 8 and 9 show peaks of the activation energy at time to 2 pct strain for *Gr. I*. This indicates that if the times to 2 pct strain are plotted in Figure 11, the slope of time to 2 pct strain for *Gr. I* would be the smallest, although the drawing is omitted in Figure 11 to avoid complexity, and obvious hardening followed by softening is thus confirmed even in *Gr. I*. However, the slope for *Gr. III'* in Figure 11 increases with the progress of creep deformation, and the hardening effect weakens gradually. The hardening in *Gr. I* and subsequent rapid softening in *Gr. III* blur the presence of *Gr. III'* in time to rupture. It is important to note from Figure 11 that there is certainly hardening in *Gr. I* and *III'* before we encounter an unexpected drop in strength for any creep time of *Gr. III* and that softening occurs within *Gr. I* and *III'* themselves after the hardening. Figures 8 and 11 show that Q of *Gr. I* peaked at 2 pct strain, and subsequently, recovery had already begun before the MCR occurred. Similar recovery was confirmed for *Gr. III'*, before the time to MCR. In other words, the presence of a peak of Q followed by recovery before the time to MCR should be a sign of an unexpected drop in strength in the future. These processes occur around 1000 hours, before there is a 0.5 pct drop in creep strength for *Gr. III*, and therefore, if we search the early stage of creep deformation in detail, we will find a sign of an unexpected strength drop in the data of time to rupture at an earlier time on the order of 1000 hours.

In the above, it was pointed out that if the creep curves of *Gr. I*, *III'*, and *III* at around 873 K (600 °C) for the high-chromium and high-strength martensitic steel were precisely investigated, a sign of an unexpected drop in rupture strength that will occur after several tens of thousands of hours should be obtained. In particular, when the data of Figure 11 are compared with Figures 8 and 9, it was found that, besides the occurrence of the abnormally low values of Q and V around 10,000 hours, peaks of Q and V —followed by recovery after only about 1000 hours, before the time to MCR—are found mainly in *Gr. I*. This should be a sign of an unexpected strength drop in the future,

although unfortunately, the sign does not tell when the unexpected strength drop will happen. However, since a newly developed steel has a target temperature, stress, and time (e.g., 100,000 hours) for rupture, it is possible that if changes in the slope, $-\partial\sigma/\partial\log t$, of a diagram of stress vs time to a specified strain, like the one of Figure 11, are investigated using creep curves under the approximate conditions of the previously determined target, a more certain sign of an unexpected strength drop that will occur in the future can be obtained, maybe within 10,000 hours.

VI. METALLURGICAL CONSIDERATIONS

A. Creep Mechanisms for *Gr. I–III'*

Reviewing creep behaviors at temperatures ranging from 873 to 923 K (600 to 650 °C) shown in Figures 2, 3, 7, and 11, it is found that hardening (*Gr. I and III'*) takes place before the occurrence of the unexpected and drastic drop in strength (*Gr. III*), and the degradation rate is mitigated in due time (*Gr. IV and V*). In this situation, hardening was observed at 873 K (600 °C) for about 1000 hours through a transition range from *Gr. I* to *Gr. III'* of the times to 0.5 and 1 pct strains and during creep deformation of *Gr. I* from about 1 pct to rupture as shown in Figure 11, where each slope changes from steep to shallow corresponding to the changes in the activation volume shown in Figure 9. Under these test conditions, the considerably high activation energy ranges from about 650 to 1000 kJ/mol as shown in Figure 8, although the activation energy of several carbon steels, low-alloy steels, and austenitic stainless steels are approximately 400 kJ/mol.^[16,17] Extremely high values of the activation energy shown in Figure 8 are considered to denote increasing resistance to moving dislocations.

The microstructure of 11Cr-2W-0.4Mo-1Cu-Nb-V steel, studied here, is tempered martensite strengthened by the precipitation of $M_{23}C_6$, MX, Laves phase and solid solution, and the addition of B.^[24] The temperature range where hardening is observed in Figure 7, i.e., from 873 K to 923 K (600 °C to 650 °C), is the temperature range of precipitation of Laves phase.^[25] A creep duration of about 1000 hours at 873 K (600 °C) is enough for the recovery of the lath-martensite structure including a decrease in dislocation density, but is not enough for the precipitation of Z phase for this steel.^[26,27] Therefore, MX particles showing a powerful strengthening effect^[27–29] have not yet decomposed, and it is thus reasonable to infer that the hardening observed in Figure 7 is not caused by something concerning the redistribution of constituent elements of MX particles, but certainly by the precipitation of Laves phase during creep. Thermal input of 873 K (600 °C) for 1000 hours is enough for this steel to precipitate Laves phase.^[25]

In a high-temperature region higher than 973 K (700 °C) (*Gr. II*), Q is as large through the whole range of creep deformation as values for *Gr. I* and *III'* as shown in Figure 8. The values of Q for time to rupture of many kinds of heat-resistant steels do not exceed

500 kJ/mol,^[16–18] although Q increases to some extent at high temperatures in some cases.^[16] In a high-temperature region higher than 973 K (700 °C), neither Laves phase nor Z phase precipitates in high-Cr martensitic steel containing Mo and/or W,^[25,29] and therefore, major strengthening factors are considered to be both W and/or Mo, most of which are soluble, and fine MX particles that precipitate stably in the martensitic matrix. Kadoya and Shimizu^[13] studied the creep behavior at 873 K (600 °C) of iron-containing soluble W and Mo and finely dispersed MX particles. The activation volumes can be calculated as 1142 and 688 cm³/mol, respectively, although the activation energy cannot be calculated because there are no other temperature data. It is found that the activation volume for creep in a solid-solution hardening state is far larger than that in a precipitation-hardening state. Figure 9 shows that the value of V for *Gr. II* is far greater than values for *Gr. I*, where precipitation and martensite hardening are considered to be the major strengthening factors. Therefore, it can be said that the major strengthening factors for *Gr. II* are soluble W and/or Mo atoms, although there is a temperature difference between Kadoya's report [873 K (600 °C)] and the current study [973 K (700 °C)].

B. Creep Mechanisms for Grs. III–V

1. The unexpected drop in strength during long-term creep test

Concerning the long-term test region of *Gr. III*, Figures 7 and 11 show that there is already degradation in the time to 0.5 pct strain for 5000 hours at 873 K (600 °C) and 120 to 110 MPa. The values of Q and V during for *Gr. III* are extremely small as shown in Figures 8 and 9. The values of Q become smaller than the activation energy for the self-diffusion of α -Fe. This indicates that creep deformation is controlled by only nonconservative motion of dislocations without any strengthening mechanisms or by mixed-typed deformation including a grain-boundary-assisted diffusion process possibly with some strengthening mechanisms. The activation volume for *Gr. III* shown in Figure 9 is also extremely small. This indicates that only an activation process with a very small displacement to deform plastically is feasible, because V is a variable proportional to the displacement of a specimen in an activation process.^[19] In general, V is understood to be proportional to the area swept by dislocations, but these dislocations cannot stay in and necessarily should move out of the specimen and/or the large-angled grains, which results in a measurable displacement, because work hardening should not occur macroscopically in the range of *Gr. III*. Total displacement is determined by the product of the number of deformable sites and the average displacement for each site. Therefore, it is most reasonable to explain the small value of V by the number of deformation sites being limited or creep progressing nonuniformly; this suggests deformation is concentrated near the grain boundaries, which is consistent with the low values of Q as mentioned above. This does not suggest grain-boundary sliding, which is

not a major deformation mechanism in the temperature range studied. In contrast, if a large number of deformation sites (*i.e.*, uniform deformation) is modeled, the displacement for each site should be limited to being extremely small. This means that resistance to dislocation motions is considerably large for *Gr. III* and leads to difficulty in understanding why Q for *Gr. III* of the material degradation data is very small, as shown in Figure 8.

2. Causes for the unexpected drop in strength

a. Z phase. Previous work on high-Cr martensitic steels has attributed the unexpected drop in strength to the formation of Z phase.^[10,11] The degradation is summarized as follows. Z phase forms in ferritic/martensitic steels containing large amounts of Cr and N, V, and Nb after long thermal exposure similar to the case for austenitic steel;^[26,30] the nose temperature of Z-phase precipitation (*i.e.*, the temperature at which precipitation occurs earliest) is 923 K (650 °C);^[27] the composition of Z phase is Cr(Nb,V)N, and small amounts of Fe and Si are dissolved;^[27,28] a thermodynamic calculation system showed that Z phase is more stable than MX in high-Cr ferritic/martensitic steel;^[30–32] the nucleation mechanism is not well understood, but Z phase easily nucleates on VN and Z phase is further stabilized by dissolving Nb;^[32–34] Nb precipitates forming MX on PAGB during normalization, and Z phase is found on PAGB near Nb containing MX;^[28,35,36] Z-phase particles grow and/or become coarse by collecting nearby Cr, and dissolving and consuming finely dispersed MX particles in grains^[35,36]; and a region several microns in width along and adjacent to PAGB on which coarse M₂₃C₆ and Z-phase particles grow is preferentially recovered, the timing of which corresponds to an unexpected and sharp drop in strength.^[10,35–37]

According to the previous work shown above, the unexpected drop in strength in the times to rupture and specified strain observed at 873 K (600 °C) after several thousands of hours for 11Cr-2W-0.4Mo-1Cu-Nb-V steel (shown in Figures 2, 7, and 11) is considered to be mainly because of the formation of Z phase on PAGB and the resulting local and heterogeneous recovery along PAGB. This inference agrees with the observation of Z phase on PAGB in a creep-ruptured specimen of this steel after 3475 hours at 873 K (600 °C).^[27] Moreover, the heterogeneous recovery model proposed by Kimura *et al.*,^[35] where glide resistance for mobile dislocations is estimated to be small, grain-boundary assisted diffusion can be expected, and creep deformation is localized, agrees well with the observed results of small values of Q and V in *Gr. III* shown in Figures 8 and 9.

The nose temperature of Z-phase formation is 923 K (650 °C) for this steel,^[28] and so, an unexpected drop in strength could occur at 923 K (650 °C) rather than 873 K (600 °C), at which the strength drop was observed most obviously as shown in Figures 2 and 7. However, the number density of Z-phase at 923 K (650 °C) does not exceed approximately one-third of that of at 873 K (600 °C).^[27] Therefore, even though

there might be local recovery due to Z-phase formation at 923 K (650 °C), the influence on degradation at 923 K (650 °C) should be understood to be limited, compared with degradation at 873 K (600 °C).

b. Laves phase. An unexpected drop in strength has been reported very often in the literature, before Z phase was found in high-Cr martensitic steel. At that time, precipitation and coarsening of Laves phase on PAGB, local exhaustion of Mo, and the resultant local recovery were considered to explain the strength drop.^[35] Such degradation may also happen in the steel considered here. Miki *et al.*^[38] explained that the coarsening of Laves phase on PAGB and other boundaries is responsible for the strength drop observed in 11.5Cr-3.5W-3Co-0.06Nb-0.15V-0.02N, which hardly forms Z phase. Moreover, the long-term rupture strength of 9Cr-4W steel, which precipitates only $M_{23}C_6$ and Laves phase and cannot form Z phase, is reported to decrease at 923 K (650 °C).^[39] As mentioned in section VI-A, the precipitation of Laves phase increases creep resistance within a short time. On the contrary, after a longer creep time, the precipitation of Laves phase on grain boundaries results in the unexpected drop in creep strength of this steel.

c. δ -ferrite. Yoshizawa *et al.*^[40] reported rupture tests performed at 923 K (650 °C) on longitudinally machined specimens of ASTM Gr.122 containing 10 pct of δ -ferrite showing that δ -ferrite reduces rupture strength. It was pointed out that the reduction in strength was because of not only the small number of MX in δ -ferrite but also the nonuniform distribution of MX. The steel pipes used in the current study certainly contain a small amount of δ -ferrite; however, the steel plates and tubes that did not contain δ -ferrite also had an obvious unexpected drop in strength. Therefore, the existence of δ -ferrite in 11Cr-2W-0.4Mo-1Cu-Nb-V steel is not considered to be a reason for the drop in strength shown in Figure 2.

3. Intrinsic strengthening factors for long-term strength of high-Cr martensitic steel

Danielsen^[32] calculated a thermally equilibrated state and precipitation kinetics for an 11Cr-2.5W-0.2Mo-3Co-Nb-V(0.10C, 0.025N, 0.013B) steel similar to the current steel at 923 K (650 °C) and reported that most of the MX is finally consumed and substituted by the Z phase. If in the current steel similar exhaustion of MX phase could occur even at around 873 K to 923 K (600 °C to 650 °C) and we assume that the martensitic structure is fully recovered and all kinds of precipitates such as $M_{23}C_6$, Laves phase, and Z phase are coarsened, the predominant strength mechanism should be only solid-solution strengthening by W and Mo at these temperatures. Indeed, in Figure 10, the relation between times to rupture and 0.5 pct strain shows that deformation mechanism of *Gr. III to V* is similar to that of *Gr. II*; *i.e.*, essentially solid-solution hardening.

From Figure 5, the rupture strength at 923 K (650 °C) after 100,000 hours can be roughly estimated as 35 MPa at least. This was true for the cases of plates

and tubes. However, the rupture strength of plain 9Cr-1Mo steel at 923 K (650 °C) after 100,000 hours is 25 MPa at most.^[41] In addition, the rupture strength of duplex 9Cr-2Mo steel at 923 K (650 °C) after 100,000 hours is about 28 MPa.^[42] W and Mo contents of the current steel are 1.89 and 0.34 pct, respectively. Mo equivalence of the currently examined steel is calculated as 1.3 pct Mo, if we assume the conversion factor for W is 0.5. Since the amounts of soluble W and/or Mo for these steels are similar to each other after the completion of the Laves phase, the differences in 100,000-hours rupture strength between currently examined steel and 9Cr-1Mo or 9Cr-2Mo steel cannot be explained only by solid-solution hardening, considering that MX particles have been consumed in the formation of Z phase.

Sawada *et al.*^[43] studied the variation in microstructure of the creep-ruptured specimens at 923 K (650 °C) within 10,000 hours for 9Cr-3W-3Co-0.06Nb-0.2V-0.06N steel and found both MX and Z phase co-existing in a ruptured specimen after about 10,000 hours. In addition, they reported that Nb and V contents in the extracted residues were approximately 100 and 50 pct of total contents, respectively. Miki *et al.*^[38] studied creep-rupture properties of 8.5-11.5Cr-3.5W-3Co-0.06Nb-0.15V steel at 923 K (650 °C) after longer than 10,000 hours and reported that chemical compositions in the extracted residues almost agreed with the thermally equilibrated values for all elements excepting V, and that vanadium contents in the residue are limited to only 60 pct of the total V content. Azuma *et al.*^[44] studied the creep behavior of 10Cr-1.8W-0.7Mo-3Co-0.2V-0.06Nb steel at 923 K (650 °C) after longer than 10,000 hours and reported that V contents in the residue are no more than 30 pct of the total V content, and that B addition reduces this percentage. Suzuki^[37] studied the creep-rupture behavior of a modified 9Cr-1Mo steel at 873 K to 973 K (600 °C to 700 °C) in detail and reported that, in the extracted residues of the ruptured specimens, about 100 pct of total Nb is precipitated, but only 76 pct of total V is in the residue on average. Suzuki^[37] also reported that only 80 pct of the average of total N was found in the extracted residues. Lundin *et al.*^[45,46] investigated the microstructure of 11C-1W-1Mo-0.04Nb-0.2V-0.06N steel employing atom-probe field-emission microscopy and reported that approximately 50 pct of total V was found in the matrix as a normalized and subsequently tempered state at 1023 K (750 °C). This observation does not contradict the experimentally obtained solubility product for VN in α -Fe,^[47] but there is a great difference in soluble V in the matrix calculated using a thermodynamic calculation system.^[48] Lundin *et al.*^[45,46] also suggested the existence of clusters or ultrafine particles composed of C, N, V, Cr, and Fe in the matrix, although the amount of VN in lath martensite was unexpectedly small, and they interpreted the phenomenon as mobile dislocations having dynamical interactions with these clusters or ultrafine particles inducing segregation of the above elements and subsequent dissolving of the clusters or ultrafine particles, which results in the so-called latent creep resistance^[49] during creep. Kubon *et al.*^[50] supported the

idea proposed by Lundin *et al.*^[45,46] Such dynamical interactions of dislocations with constituent elements of MX are not a rare case; sequential events of precipitation on dislocations, energetic destabilization of the precipitated particles through the breaking away of dislocations, and the subsequent dissolution of precipitated particles are well recognized in the tempering of high-Cr heat-resistant steels.^[51-54] These phenomena can be explained thermodynamically, and therefore, besides the MX particle, fine particles of not only ϵ -carbide^[55] and $M_{23}C_6$ ^[56] but also even the stable oxide $Y_2Ti_2O_7$ ^[57] have been found to be easily dissolved in interactions with dislocations.^[58]

That is, it is clear that when we discuss the creep deformation of heat-resistant steel, we should take the local equilibrium around mobile dislocations into account, and microstructural considerations based on a simple thermal equilibrium and/or kinetic simulation are insufficient. From the above discussion, it is well understood that the creep resistance of high-Cr-Mo, W heat-resistant steels that contain both V and N to some extent is superior to that of 9Cr-1Mo steel, and therefore, the long-term rupture strength of currently examined steel is not lowered as the levels of 9Cr-1Mo steel and remains at certain levels after the occurrence of the unexpected drop in strength for *Gr. III*.

4. Recovery of degradation

The transition of the slope of a diagram of stress vs time to rupture or a specified strain which corresponds to the changes in the deformation mechanism, from *Gr. III* to *Gr. IV* and/or *V* occurs not only at temperatures higher than 873 K (600 °C) but also should occur after a long time holding at 873 K (600 °C) as shown in Figures 2, 7, and 11. The width of the depleted zone of fine particles of MX and soluble W and/or Mo due to the formation of Z phase and Laves phase near large-angle boundaries is expanded to the center of grains with the progression of creep. Therefore, deformations of *Grs. IV* and *V* develop uniformly in contrast to the case for *Gr. III*, which results in decrease in the contribution of grain-boundary-assisted diffusion. These events cause increases in the activation volume and energy. At higher temperatures, *i.e.*, *Grs. IV* and *V*, solubilities of W and/or Mo increase and therefore, the activation energy increases further in *Grs. IV* and *V* compared with *Gr. III*. In any event, the degradation rate will slow down during longer-term creep and/or higher temperature creep, because the exhausted region of Mo and/or W extends into grains and a uniform microstructure forms after longer time. However, it is noticed that the strength level of this steel is not lowered to those of the plain Cr-Mo steels, but the strength levels of the high-Cr and high-strength martensitic steels can hold at least higher levels than those of the plain Cr-Mo steels due to the dynamic interactions between mobile dislocations and solute atoms such as V and N.

C. Alloy Improvement

The main reasons for the unexpected strength drop in the long-term rupture test shown in Figure 2 are that

important strengthening factors are lost near PAGB and other boundaries within a short time, and the subsequent recovered regions form locally and rapidly. However, there were obvious differences in the degradation behaviors of the three steel products. The differences may be because of a synthetic combination of not only the differences in chemical composition but also in heat treatment, segregation, and the rolling schedule. Therefore, improvements may prevent to some extent an unexpected drop in strength and increase the long-term rupture strength.

VII. CONCLUSIONS

The study analyzed current long-term rupture data for 11Cr-2W-0.4Mo-1Cu-Nb-V steel to establish an adequate fitting equation for the data and a method of estimating the long-term rupture strength. Further, a method for detecting a sign of a decrease in the long-term strength was also studied, and the following conclusions were obtained.

- (1) The rupture strength of the studied steel decreased rapidly against logarithmic time at around 873 K (600 °C) after more than 10,000 hours accompanying material degradation; however, this abrupt drop in strength tends to be moderated at higher temperatures and/or by a longer time of creeping.
- (2) To estimate the long-term rupture strength of materials that will degrade after a long time, it is necessary to use data including sufficient number of rupture-life data corresponding to the degradation and classify the data into several data groups according to the deformation mechanism.
- (3) An adequate fitting equation for the classified data is of exponential type:

$$t_r = t_{r0} \exp[(Q - \sigma V)/RT],$$

where t_r , σ , T , and R are the time to rupture, the applied stress, the absolute temperature, and the gas constant, respectively; t_{r0} is a constant; Q is the activation energy; and V is the activation volume. This equation is based on the assumption of a thermal activation process to the time to rupture, and metallurgical considerations can be taken into account in estimating long-term strength.

- (4) It is desirable to analyze creep curves in detail (for example, the time to 0.5 pct strain) to detect a sign of the long-term strength drop from short-term data.
- (5) Both the activation energy and volume for the occurrence of an unexpected and drastic strength drop are extremely small, which indicates that deformable regions are fully recovered and localized.
- (6) These locally recovered regions extend over a wide range at higher temperatures, and after a longer time the microstructure approaches uniformity, which reduces the degradation tendency. The rupture strength of this state is considered to be much higher than that of a state estimated using thermodynamic calculation systems. This means that the

dynamic interactions between solute atoms and dislocations should be taken into account when considering the long-term creep of high-Cr high-strength martensitic steel.

TABLE OF SYMBOLS

Q	Activation energy or increase in internal energy owing to creep deformation
Q'	Apparent activation energy
V	Activation volume
C	Larson–Miller constant
R	Gas constant
T	Absolute temperature
P	Larson–Miller parameter
R_{mtr}	Estimated maximum time-to-rupture ratio
t_{r0}	Constant of Eq. [1]
t_r	Time to rupture
t	Time to strain
σ	Applied stress

REFERENCES

- V.K. Sikka, C.T. Word, and K.C. Thomas: *Ferritic Steels for High Temperature Applications*, A.K. Khavne, ed., ASM Int., Metals Park, OH, 1983, pp. 65–84.
- F. Masuyama: *ISIJ Int.*, 2001, vol. 41, pp. 612–25.
- F. Masuyama: *Int. J. Press. Vessel Pip.*, 2007, vol. 84, pp. 53–61.
- F.R. Larson and J. Miller: *Trans. ASME*, 1952, vol. 74, pp. 765–75.
- NIMS CREEP DATA SHEET (0.2C, JIS STB 410, tubes), No. 7B, C. Tanaka, ed., National Institute for Materials Science (NIMS), Tsukuba, 1992, pp. 1–23.
- J. Glen and R.R. Barr: *High Temperature Properties of Steels, 1966, Proc. of the Joint Conf. Organized by the British Iron and Steel Research Association and the Iron and Steel Institute at the Grand Hotel Eastbourne*, ISI Publication 97, The Iron and Steel Institute, London, 1967, pp. 225–26.
- S. Yokoi, N. Shinya, H. Kushima, and H. Tanaka: *Tetsu-to-Hagane*, 1982, vol. 68, pp. 982–88.
- K. Kimura, H. Kushima, K. Yagi, and C. Tanaka: *Tetsu-to-Hagane*, 1991, vol. 77, pp. 667–74.
- F. Abe: *Ferrum*, 2006, vol. 11, pp. 197–207.
- H. Kushima, K. Kimura, and F. Abe: *Tetsu-to-Hagane*, 1999, vol. 85, pp. 841–47.
- K. Suzuki, S. Kumai, H. Kushima, K. Kimura, and F. Abe: *Tetsu-to-Hagane*, 2000, vol. 86, pp. 550–57.
- V. Sklenicka, K. Kucharova, M. Svoboda, L. Kloc, J. Bursik, and A. Kroupa: *Mater. Character.*, 2003, vol. 51, pp. 35–48.
- Y. Kadoya and E. Shimizu: *Tetsu-to-Hagane*, 1999, vol. 85, pp. 827–34.
- K. Kimura, K. Sawada, K. Kubo, and H. Kushima: *ASME-PVP*, 2004, vol. 47, pp. 11–18.
- NIMS CREEP DATA SHEET (11Cr-2W-0.4Mo-1Cu-Nb-V, KA-SUS 410J3 TP, pipes, KA-SUS 410J3, plates, and KA-SUS 410J3 TB, tubes), No. 51A, T. Ogata, ed., NIMS, Tsukuba, 2013, pp. 1–54.
- M. Tamura, F. Abe, K. Shiba, H. Sakasegawa, and H. Tanigawa: *Metall. Mater. Trans. A*, 2013, vol. 44A, pp. 2645–61.
- M. Tamura, H. Esaka, and K. Shinozuka: *ISIJ Int.*, 1999, vol. 39, pp. 380–87.
- M. Tamura, H. Esaka, and K. Shinozuka: *Mater. Trans.*, 2003, vol. 44, pp. 118–26.
- T. Mura and T. Mori: *Maikuromekanikkusu (Micromechanics)*, Tokyo, Baihu-kan, 1976, pp. 99–108.
- F.H. Norton: *The Creep of Steel at High Temperatures*, McGraw-Hill Book Co., New York, 1929, pp. 1–90.
- H. Oikawa: *The Technology Reports of the Tohoku University*, Tohoku University, Sendai, 1982, vol. 47, pp. 67–77.
- F.C. Monkman and N.J. Grant: *ASTM*, 1956, vol. 56, pp. 593–620.
- A.H. Sully: *Metallic Creep and Creep Resistant Alloys*, Butterworths Scientific Pub, London, 1949, pp. 37–57.
- A. Iseda, Y. Sawaragi, S. Kato, and F. Masuyama: *5th Int. Conf. on Creep of Materials, Creep: Characterization, Damage and Life Assessment*, 1992, ASM, Materials Park, pp. 389–98.
- F. Abe, H. Araki, and T. Noda: *Metall. Trans. A*, 1991, vol. 22A, pp. 2225–35.
- A. Strang and V. Vodarek: *Mater. Sci. Technol.*, 1996, vol. 12, pp. 552–56.
- K. Sawada, H. Kushima, K. Kimura, and M. Tabuchi: *ISIJ Int.*, 2007, vol. 47, pp. 733–39.
- K. Sawada, H. Kushima, and K. Kimura: *ISIJ Int.*, 2006, vol. 46, pp. 769–75.
- H.K. Danielsen and J. Hald: *Energy Mater.*, 2006, vol. 1, pp. 49–57.
- H.K. Danielsen and J. Hald: *VGB Power Technol.*, 2009, vol. 5, pp. 68–73.
- C. Kocer, T. Abe, and A. Soon: *Mater. Sci. Eng. A*, 2009, vol. 505, pp. 1–5.
- H.K. Danielsen: Ph.D. Thesis, 2007, Technical University of Denmark.
- A. Golpayegani, H.-O. Andren, H. Danielsen, and J. Hald: *Mater. Sci. Eng. A*, 2008, vol. 489, pp. 310–18.
- R.O. Kaibyshev, V.N. Skorobogatykh, and I.A. Schenkova: *Metal Sci. Heat Treatment*, 2010, vol. 52, pp. 90–99.
- K. Kimura, H. Kushima, and F. Abe: *Key Eng. Mater.*, 2000, vols. 171–174, pp. 483–90.
- K. Kimura, K. Suzuki, Y. Toda, H. Kushima, and F. Abe: *Proc. 7th Liege Conf. on Mater. For Advanced Power Eng. 2002*, Forschungszentrum, Julich, 2002, pp. 1171–80.
- K. Suzuki: Dr. Thesis, 2002, Tokyo Institute of Technology.
- K. Miki, T. Azuma, T. Ishiguro, R. Hashizume, Y. Murata, and M. Morinaga: *Proc. 7th Liege Conf. on Mater. For Advanced Power Eng. 2002*, Forschungszentrum, Julich, 2002, pp. 1497–504.
- F. Abe: *Metall. Mater. Trans. A*, 2005, vol. 36A, pp. 321–32.
- M. Yoshizawa and M. Igarashi: *Proc. Int. Conf. on Creep and Fracture in High Temperature Components*, Destech. Pub., London, 2005, pp. 110–18.
- NIMS CREEP DATA SHEET (JIS STBA 2, 9Cr-1Mo, tubes), No. 19B, H. Irie, ed., NIMS, Tsukuba, 1997, pp. 1–29.
- NIMS CREEP DATA SHEET (KA-STBA 27, 9Cr-2Mo, tubes), No. 46A, S. Matsuoka, ed., NIMS, Tsukuba, 2005, pp. 1–15.
- K. Sawada, M. Taneike, K. Kimura, and F. Abe: *ISIJ Int.*, 2004, vol. 44, pp. 1243–49.
- T. Azuma, K. Miki, Y. Tanaka, and T. Ishiguro: *Tetsu-to-Hagane*, 2002, vol. 88, pp. 678–85.
- L. Lundin, M. Norell, H.-O. Andren, and L. Nyborg: *Scand. J. Metall.*, 1997, vol. 26, pp. 27–40.
- L. Lundin, S. Fallman, and H.-O. Andren: *Mater. Sci. Technol.*, 1997, vol. 13, pp. 233–42.
- K. Narita, S. Koyama, and T. Ishii: *Tekkokuikokuyodokenkyukai, V-kenkyukai-kyodohokokusho*, ISIJ, Tokyo, Biryogensobukai, 1970, pp. 1–15.
- B. Sundman, B. Jansson, and J.-O. Andersson: *CALPHAD*, 1985, vol. 9, pp. 153–90.
- J. Glen: *J. Iron Steel Inst.*, 1958, vol. 189, pp. 333–43.
- Z. Kubon, V. Foldyna, and V. Vodarek: *Microstructural Stability of Creep Resistant Alloys for High Temperature Plant*, A. Strang, T. Canley, and G.W. Greenwood, eds., Institute of Materials, London, 1998, pp. 257–70.
- M. Tamura, K. Ikeda, H. Esaka, and K. Shinozuka: *ISIJ Int.*, 2001, vol. 41, pp. 908–914.
- M. Tamura, H. Iida, H. Kusuyama, K. Shinozuka, and H. Esaka: *ISIJ Int.*, 2004, vol. 44, pp. 153–61.
- M. Tamura, H. Kusuyama, K. Shinozuka, and H. Esaka: *ISIJ Int.*, 2007, vol. 47, pp. 317–26.
- M. Tamura, M. Nakamura, K. Shinozuka, and H. Esaka: *Metall. Mater. Trans. A*, 2008, vol. 39A, pp. 1060–76.
- M. Cohen: *Trans. JIM*, 1968, vol. 9 Supplement, pp. XXIII–XXIX.

56. M. Tamura, Y. Haruguchi, M. Yamashita, Y. Nagaoka, K. Ohinata, K. Ohnishi, E. Itoh, H. Ito, K. Shinozuka, and H. Esaka: *ISIJ Int.*, 2006, vol. 46, pp. 1693–702.

57. M. Tamura, H. Sakasegawa, K. Shiba, H. Tanigawa, K. Shinozuka, and H. Esaka: *Metall. Mater. Trans. A*, 2011, vol. 42A, pp. 2176–88.

58. M. Tamura: *Ferrum*, 2009, vol. 14, pp. 17–22.